Preclinical and 'near-patient' models for the evaluation of experimental therapy in prostate and bladder cancer

Merbel, A.F. van de

6 Reovirus Mutant *jin-3* Exhibits Lytic and Immune-Stimulatory Effects in Preclinical Human Prostate Cancer Models

Arjanneke F. van de Merbel
Geertje van der Horst
Maaike H. van der Mark
Selas T. F. Bots
Diana J. M. van den Wollenberg
Corrina M. A. de Ridder
Debra Stuurman
Tilly Aalders
Sigrun Erkens-Schulz
Nadine van Montfoort
Wouter R. Karthaus
Niven Mehra
Minke Smits
Jack A. Schalken
Wytske M. van Weerden
Rob C. Hoeben
Gabri van der Pluijm

Cancer Gene Therapy (2021)

Abstract

Treatment of castration-resistant prostate cancer remains a challenging clinical problem. Despite the promising effects of immunotherapy in other solid cancers, prostate cancer has remained largely unresponsive. Oncolytic viruses represent a promising therapeutic avenue, as oncolytic virus treatment combines tumour cell lysis with activation of the immune system and mounting of effective anti-tumour responses. Mammalian Orthoreoviruses are non-pathogenic human viruses with a preference of lytic replication in human tumour cells. In this study, we evaluated the oncolytic efficacy of the bioselected oncolytic reovirus mutant *jin-3* in multiple human prostate cancer models. The *jin-3* reovirus displayed efficient infection, replication, and anti-cancer responses in 2D and 3D prostate cancer models, as well as in ex vivo cultured human tumour slices. In addition, the *jin-3* reovirus markedly reduced the viability and growth of human cancer cell lines and patient-derived xenografts. The infection induced the expression of mediators of immunogenic cell death, interferon-stimulated genes, and inflammatory cytokines. Taken together, our data demonstrate that the reovirus mutant *jin-3* displays tumour tropism, and induces potent oncolytic and immunomodulatory responses in human prostate cancer models. Therefore, *jin-3* reovirus represents an attractive candidate for further development as oncolytic agent for treatment of patients with aggressive localised or advanced prostate cancer.

Introduction

Prostate carcinoma is the second most common cancer and the fifth leading cause of cancer-related death in men worldwide (1). The development of therapy resistance and incurable metastatic disease represents major clinical problems. Immunotherapy has emerged as a viable and attractive strategy for the treatment of different solid cancers (2). Despite the success of immunotherapeutic approaches in various cancers, prostate cancer has remained largely unresponsive for single-agent immune therapies, including cancer vaccines and immune checkpoint inhibitors (3). Accumulating evidence suggests that prostate cancer cells escape from immune surveillance by creating an immune-suppressive and immune-exclusive tumour microenvironment (4). This immunosuppressive barrier impairs the generation and maintenance of a clinically desired anti-tumour immune response. Treatment modalities that overcome this immunosuppressive state could represent a promising option for prostate cancer.

Oncolytic viruses specifically infect, replicate, and lyse malignant tumour cells, while minimising harm to normal cells. Moreover, oncolytic viruses have the ability to promote adaptive and innate immune responses upon infection and killing of cancer cells, e.g., mediated by the release of danger-associated molecular patterns (DAMPs) like high mobility group box 1 (HMGB1) (5-8). Previously, we have demonstrated that the oncolytic potency of mammalian Orthoreoviruses can be enhanced by natural selection and genetic modification (9, 10). Reoviruses are double-stranded RNA viruses and have not been associated with severe disease in humans (11). Wild-type reovirus type 3 Dearing (T3D) has oncolytic properties in a variety of tumour types. It binds to a cancer cell by interaction of viral spike protein Sigma-1 to sialic acids and to junction adhesion molecule A (JAM-A) (10, 12, 13). However, JAM-A expression is often reduced in solid cancers and this correlates with a poor survival and a worse prognosis (14).

Mutant reoviruses with enhanced tumour tropism, that can also infect cancer cells independently of JAM-A (i.e., via negatively charged sialic acids) represent a promising treatment modality (10). Our group has generated spontaneous reovirus mutants (i.e., *jin-1*, *−2*, and *−3*) with extended tropism. These reovirus mutants are able to infect a wide range of cell lines that normally resist wild-type reovirus T3D infection (10). In the absence of JAM-A, these reovirus mutants depend on negatively charged sialic acids on the cell surface for infection.

In this study, the direct oncolytic and indirect immunomodulatory effects of *jin-3* reovirus were determined in state-of-the-art preclinical prostate cancer models, including monolayer and three-dimensional cell cultures, ex vivo cultured human prostate cancer tissue slices, and cell line and patient-derived prostate cancer xenograft models in vivo (15).

Material and methods

Virus production

Wild-type T3D reovirus strain R124 was plaque purified from the wild-type reovirus T3D (ATCC, Manassas, VA, United States) on HER911 cells [10, 16]. Reovirus mutant *jin-3* was isolated from JAM-A-deficient U118MG cells after passaging of the wild-type T3D strain R124 (10). Both R124 and *jin-3* reoviruses were propagated, purified, and titrated on human HER911 cells as described (10). Cell lines were propagated for no >6 months or 30 passages after resuscitation from stocks. All cell lines were frequently tested for Mycoplasma infection, using a Mycoplasma-specific polymerase chain reaction (PCR).

Two- and three-dimensional prostate cancer cultures

Human prostate cancer cell lines PC-3M-Pro4luc2, DU145, and 22Rv1 were cultured in monolayers (**Supplementary table 1**). Three-dimensional cultures were generated from a previously established three-dimensional prostate cancer model from bone metastasis material (MSK-PCa1), or generated from newly established patient-derived xenograft (PDX) models from prostate cancer bone and liver metastases biopsies (NM78 and NM72) (17, 18). Three-dimensional cultures of prostate cancer bone and liver metastases were maintained, as previously described (17, 18).

Viability assays

For cell lines, 1500 cells were seeded per well in a 96-well plate. After 24 h, cells were exposed to oncolytic reovirus at a multiplicity of infection (MOI) of 0.01–0.1–1–10 and 100 plaque forming units (p.f.u.)/cell. After 24 h, the medium was refreshed. After 6 days, the viability of the cells was assessed by performing MTS assays (19). Three-dimensional prostate cancer cultures were treated with oncolytic reovirus for 3, 7, and 10 days. Changes in viability were assessed by the Cell Titer Glo assay, according to the manufacturer's protocol (Promega, Madison, WI, United States).

FACS analyses

Flow cytometry was performed with LSRII (BD Biosciences, Franklin Lakes, NJ, United States) and analysed with FCS express software after staining the cells with JAM-A antibody (**Supplementary table 2**).

Sigma-3 immunocytochemistry

A total of 20,000 prostate cancer cells were seeded in eight-well chamber slides (ThermoFisher Scientific, Waltham, MA, United States). After 24 h, the cells were exposed to oncolytic reovirus After 1, 2, and 3 days of post exposure, Sigma-3 was visualised by immunofluorescence (**Supplemenatary table 2**) and confocal microscopy.

Generation of prostate cancer patient-derived xenograft models and ex vivo tumour tissue slice culture

Prostate cancer tissue was obtained via either transurethral resection of the prostate (prostatectomy) or needle biopsies after informed consent (Pronet p05.85 and RBUT-ID-PROSTAAT-151; **Supplementary table 3**). In order to establish new prostate cancer PDX models, tumour pieces were implanted subcutaneously in adult male immunodeficient mice. All animal experiments were performed after approval by the Animal Welfare Committee of the Leiden University Medical Center in accordance with the Dutch Act on Animal experimentation and EU Directive 2010/63/EU (project licenses from Central Authority for Scientific Procedures on Animals (CCD): AVD1160020173725 and AVD1160020187004). Established and well-characterised prostate cancer PDX models were propagated as described (project license AVD101002017867) (20) (**Supplementary table 4**). Tumour growth was monitored by caliper measurements. All mice were housed under sterile conditions in accordance with Dutch guidelines. Prostate cancer tissue was sliced and cultured, as previously described (19). Slices were exposed to 10^8 p.f.u./ml *jin-3* reovirus. Three days post exposure, the tissues were fixed with 4% PFA and processed for histology.

Histology and Sigma-3 scoring

H&E and immunofluorescent stainings were executed, as previously described (**Supplementary table 2**) (19). H&E-stained sections were analysed and Sigma-3-stained tumour cells were scored with the Pannoramic MIDI slide scanner (3DHISTECH, Budapest, Hungary). All fluorescently stained cells or tissue sections were visualised by confocal microscopy (63× magnification, resolution 1024 × 1024; Leica SP8, Wetzlar, Germany). Slide scans from Sigma-3 stainings were scored.

Four sections were scored per condition for positive Sigma-3 staining by two independent reviewers (**Supplementary figure 1**).

Real-time quantitative polymerase chain reaction (RT-qPCR)
Cells were seeded in six-well plates and exposed to oncolytic reovirus for 6, 24, and 48 h. Total RNA was isolated according to the manufacturer's protocol (Nucleospin RNA kit Macherey-Nagel, Düren, Germany). cDNA was generated by using random primers (Promega, Madison, WI, United States) and RT-qPCR was performed with GoTaq Mastermix (Promega, Madison, WI, United States), according to the manufacturer's protocol in technical duplicates and biological triplicates (Promega, Madison, WI, United States). Gene expression was normalised to GAPDH expression. The sequences of the PCR primers used for the quantitation of cellular transcripts, viral RNA, and the detection of mycoplasma contamination can be found in **Supplementary table 5**.

High mobility group box 1 release
Cells were exposed to oncolytic reovirus with a MOI of 10. At 48 h post exposure, conditioned medium was collected. HMBG1 release was measured by performing an ELISA, according to the manufacturer's protocol (IBL International, Hamburg, Germany).

Administration of jin-3 reovirus in vivo
Subcutaneous PC-3M-Pro4luc2 tumours were generated in male NSG mice (AVD1160020173725 and AVD1160020187004) (19). When tumours reached a volume of 0.11 cm^3, intra-tumoural administration with 10^8 p.f.u. *jin-3* reovirus in 10 µl PBS was initiated twice a week (n = 6 per group). For sample size calculations and in/exclusion criteria, see **Supplementary information.** Tumour growth was monitored by bioluminescence imaging (21). Tumour pieces of PDX model PCa-15.01 were implanted subcutaneously in the flank of male NSG mice (AVD1160020173725 and AVD1160020187004). When tumours reached a volume of 0.11 cm^3, mice were randomised based on body weight, tumour burden, and/or tumour size. Subsequently, tumours were treated by intra-tumoural injections of 10^8 p.f.u. *jin-3* reovirus (n = 10 per group). Tumour growth was assessed by caliper measurements.

Statistical analyses

Statistical analyses were performed by using GraphPad Prism 8.0. One-way ANOVA was performed for viability experiments. All in vitro experiments were repeated at least twice. Data are represented as mean ± standard error of the m ean (SEM). Two-way ANOVA and two-sided t tests were performed on data from in vivo experiments. *$p < 0.05$, **$p < 0.01$, ***$p < 0.001$, and ****$p < 0.0001$.

Results

Direct oncolytic effects of reovirus mutant jin-3 reovirus in vitro

Prostate cancer cells PC-3M-Pro4luc2, DU145, and 22Rv1 were exposed to R124 and *jin-3* reoviruses, and viral infection was monitored by RT-qPCR and confocal microscopy. Dose-dependent and time-dependent reoviral infection was observed upon exposure to R124 and *jin-3* reovirus (**Figure 1A** and **1B**).

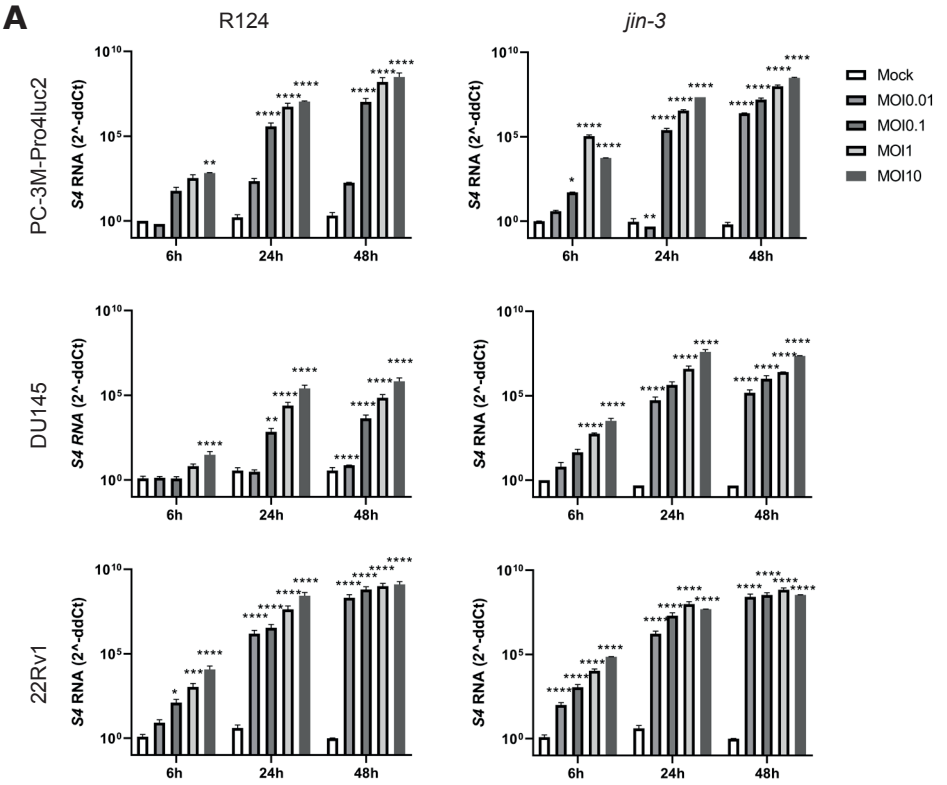

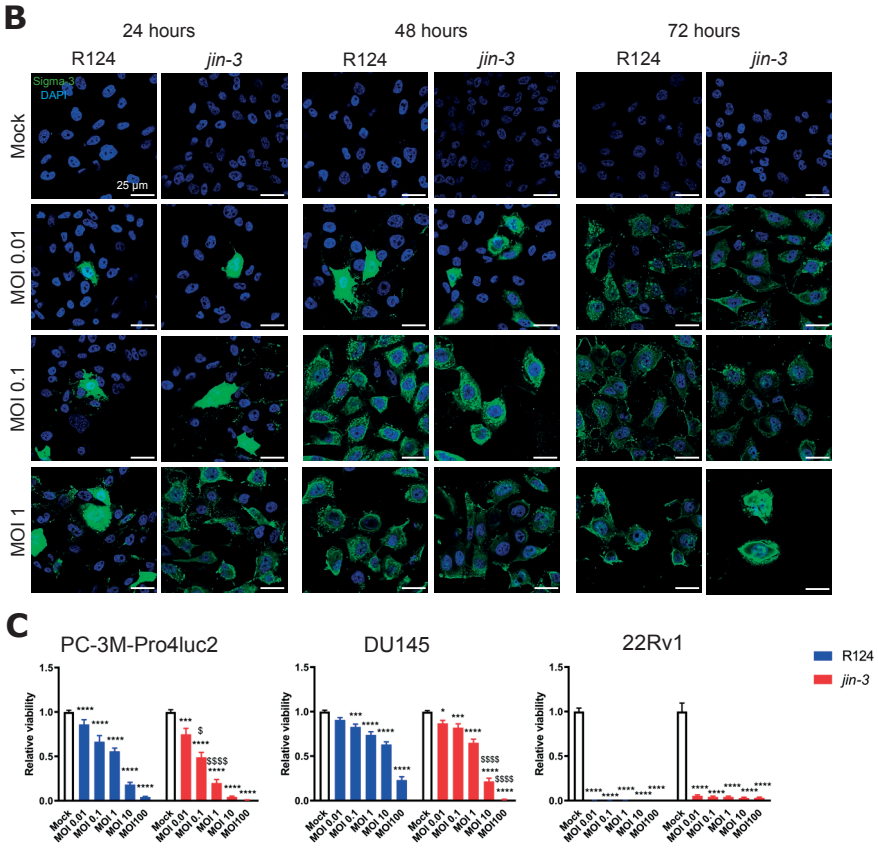

Figure 1 Infection, replication, and oncolytic effects of reovirus *jin-3* mutant versus wild-type R124 parental reovirus in prostate cancer cell lines in vitro.

*(**A**) Detection of viral transcripts (capsid protein S4) by RT-qPCR indicated dose- and time-dependent infection and replication of R124 reovirus (upper row) and jin-3 reovirus (bottom row) in human prostate cancer cells PC-3M-Pro4luc2, DU145, and 22Rv1. Gene expression is represented as $2^{-ddCt} \pm$ standard error of the mean (SEM), N = 3. Two-way ANOVA. MOI = multiplicity of infection. *p < 0.05, **p < 0.01, ***p < 0.001, ****p < 0.0001. * mock versus reovirus infection. (**B**) Confocal microscopy for Sigma-3 viral capsid protein (green) in PC-3M-Pro4luc2 cells indicated dose-dependent and time-dependent immunofluorescent localisation of Sigma-3 viral capsid protein (green) in PC-3M-Pro4luc2 prostate cancer cells that were exposed to R124 wild-type and jin-3 reoviruses. Green Sigma-3 viral capsid protein, blue DAPI (nuclei). Magnification is 63×, scale bar = 25 µm. (**C**) Dose-dependent killing of human PC-3M-Pro4luc2, DU145, and 22Rv1 prostate cancer cell lines (cell viability) upon exposure of these cells with R124 wild-type and jin-3 reoviruses for 6 days. *p < 0.05, ***p < 0.001, ****p < 0.0001, $p < 0.05, $$$$p < 0.0001. * mock versus reovirus infection, $ R124 versus jin-3. Mean ± standard error of the mean (SEM), N = 3. Two-way ANOVA. MOI multiplicity of infection*

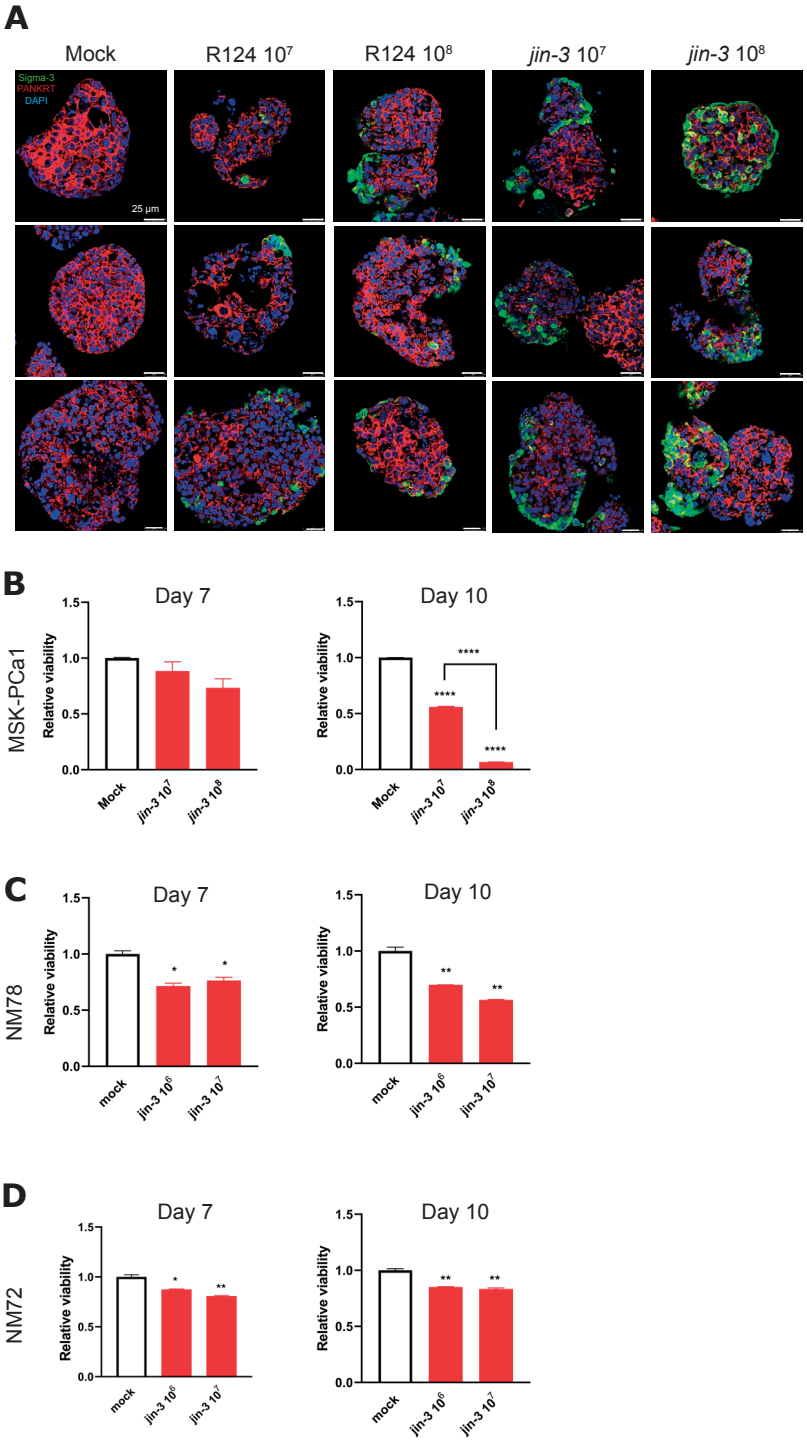
A
Mock
R124 10⁷
R124 10⁸
jin-3 10⁷
jin-3 10⁸
Sigma-3
PANKRT
DAPI
25 µm
B
MSK-PCa1
Day 7
Day 10
Relative viability
Mock
jin-3 10⁷
jin-3 10⁸
C
NM78
mock
jin-3 10⁶
jin-3 10⁷
D
NM72

Next, viability assays were performed in AR-negative prostate cancer cell lines PC-3M-Pro4luc2 and DU145 cells and AR-positive 22Rv1 cells. *Jin-3* reovirus significantly reduced the viability of all prostate cancer cell lines (**Figure 1C**). 22Rv1 cells were extremely sensitive to reovirus exposure, whereas AR-negative cell lines DU145 and PC-3M-Pro4luc2 displayed a dose-dependent decrease in viability after exposure to jin-3 (**Figure 1C**). When compared to PC-3M-Pro4luc2 and DU145 cells exposed to R124 reovirus, the viability of *jin-3* reovirus exposed PC-3M-Pro4luc2 and DU145 cells was significantly reduced ($^{\$}p < 0.05$ and $^{\$\$\$\$}p < 0.0001$ MOI1 and MOI10 in PC-3M-Pro4luc2, and $^{\$\$\$\$}p < 0.0001$ MOI10 and MOI100 in DU145; **Figure 1C**). FACS analyses revealed that 98%, 97%, and 89% of PC-3M-Pro4luc2, DU145, and 22Rv1 cells expressed JAM-A protein, respectively.

Treatment of three-dimensional cultures of bone metastasis derived MSK-PCa1 cells (17) with oncolytic reovirus revealed a dose-dependent infection and viral replication (**Figure 2A**). In addition, treatment with *jin-3* reovirus significantly decreased the viability of three-dimensional cultures of prostate cancer bone and liver metastases (MSK-PCa1, NM78, and NM72) after 7 and 10 days ($*p < 0.05$, $**p < 0.01$, $****p < 0.0001$, **Figure 2B-D**, respectively).

◄ Figure 2 Reovirus infection and replication in three-dimensional cultures of human prostate cancer.

*(**A**) Three-dimensional cultures from MSK-PCa1 prostate cancer cells, derived from a bone metastasis (17) were exposed to 10^7 and 10^8 plaque forming units (p.f.u.) of R124 or jin-3 reovirus. After 3 days, staining for reovirus (Sigma-3) was observed in the outer cell layers of the 3D cultures, indicating active viral infection and replication. Green Sigma-3 (viral protein), red pan-cytokeratin (tumour cells), blue DAPI (nuclei). Magnification is 63×, scale bar = 25 µm.(**B-D**) Three-dimensional cultures of metastatic human prostate cancer were generated and exposed to jin-3 reovirus for 7 and 10 days. Viability assays indicated a significant reduction of cellular viability after exposure to jin-3. Mean ± standard error of the mean (SEM), $*p < 0.05$, $**p < 0.01$, $****p < 0.0001$. One-way ANOVA.*

Reovirus infection and replication in ex vivo cultured prostate cancer tissue slices
Prostate cancer tissue slices were generated from explanted PC-3M-Pro4luc2 tumours and infected with *jin-3* reovirus for 2, 3, 4, and 7 days. Exposure to *jin-3* reovirus resulted in a time-dependent increase in Sigma-3 score indicating viral infection and replication (**Supplementary figure 1** and **Figure 3A** and **B**).

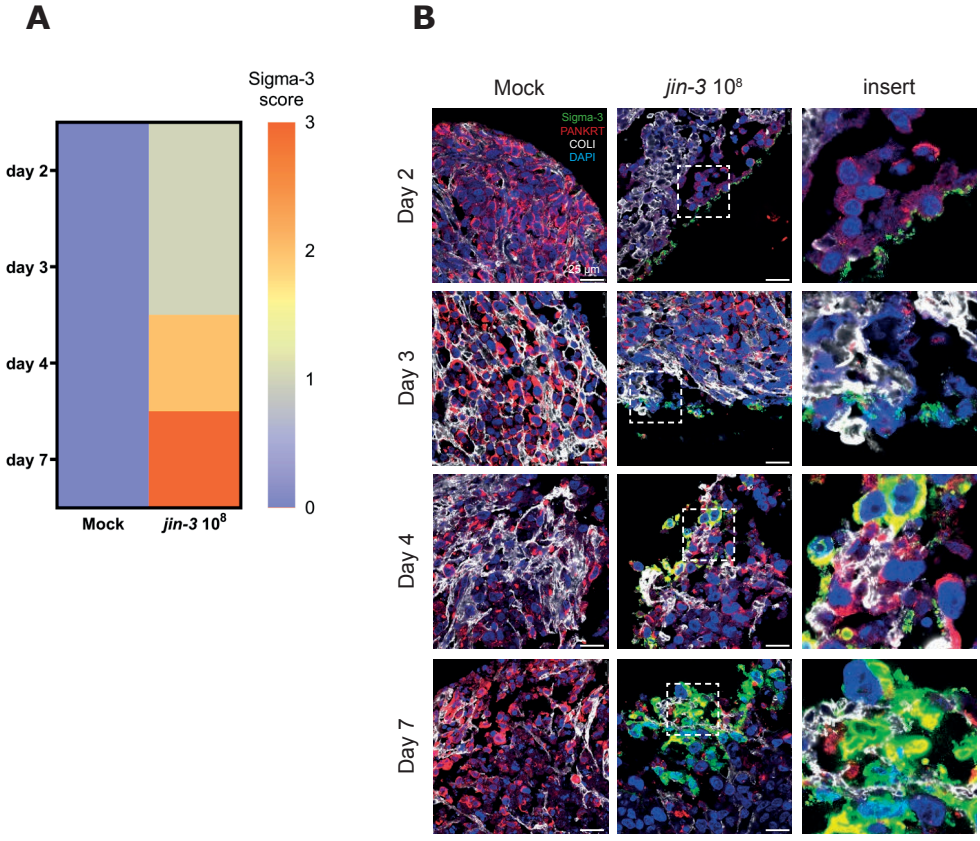

Figure 3 *jin-3* reovirus infection in ex vivo cultured tumour tissue slices from human prostate cancer cell line-derived xenografts.

*(**A**) Prostate cancer tissue slices from PC-3M-Pro4luc2 tumours were exposed to 10^8 p.f.u. jin-3 reovirus for 2, 3, 4, or 7 days. Scoring of Sigma-3 viral protein indicated a time-dependent increase in Sigma-3 score. (**B**) Viral infection and replication in ex vivo cultured tissue slices with reovirus. Green Sigma-3 (viral protein), red pan-cytokeratin (tumour cells), blue DAPI (nuclei). Magnification is 63×, scale bar = 25µm.*

Next, tumour tissue slices were generated from novel and previously established PDX models (20, 22, 23) followed by exposure to jin-3 reovirus for 3 days (**Figure 4A**). For the duration of the ex vivo tissue culture experiment, Sigma-3 staining was observed in 91% (10/11) of the PDX models in the *jin-3* reovirus-treated group (**Figure 4A** and **Supplementary figure 2**). JAM-A protein expression was observed in all PDX tumours, but the subcellular localisation of JAM-A protein varies per patient-derived tumour (**Supplementary figure 3A**). Reovirus infection was observed in both AR-positive and AR-negative PDX models (**Supplementary figure 3B**). In ex vivo cultured tissue slices from patient biopsy material, Sigma-3 staining was observed in all prostate cancer biopsies after *jin-3* reovirus exposure for 3 days (**Figure 4B** and **Supplementary figure 4**).

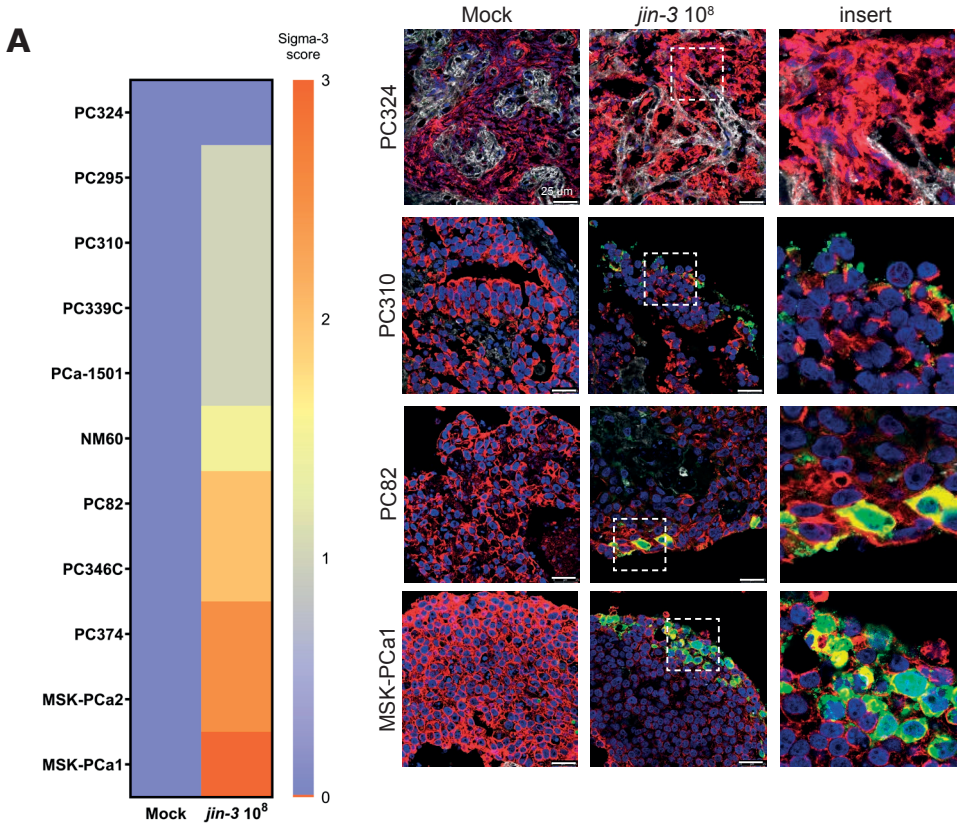

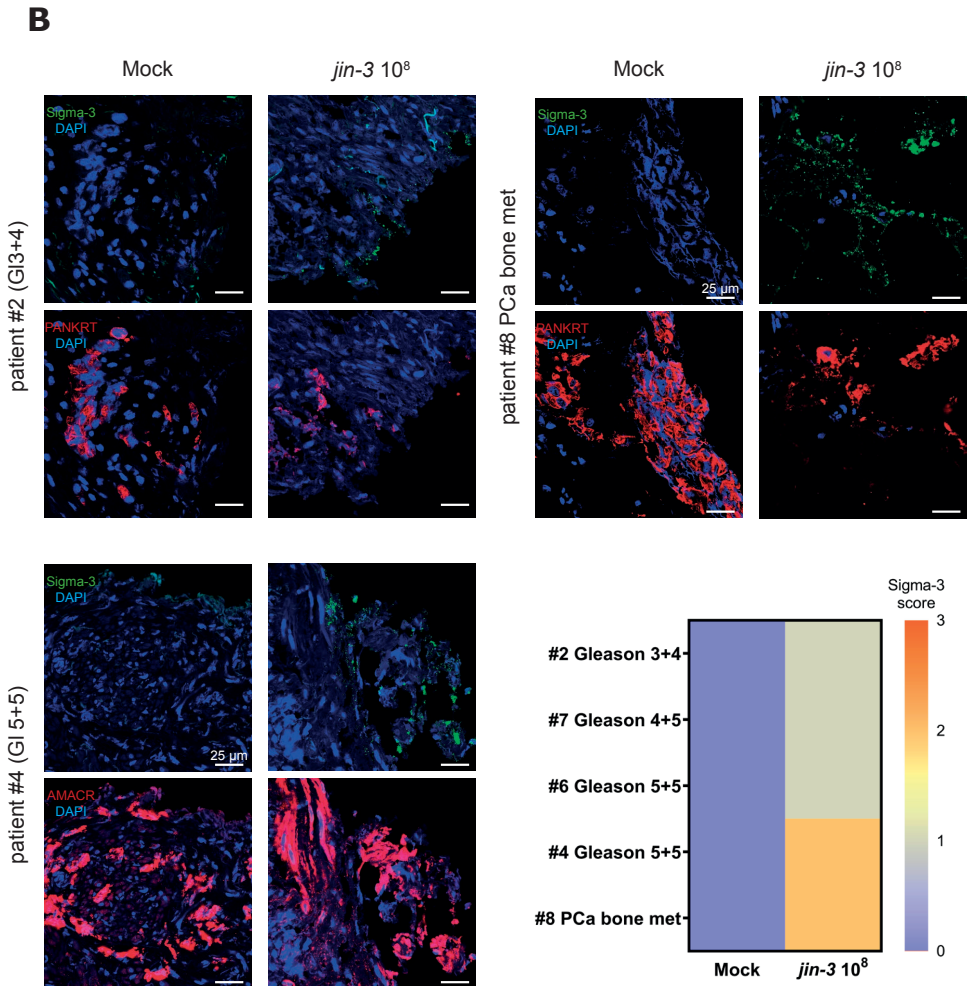

Figure 4 *jin-3* reovirus infection in prostate cancer tissue slices derived from patient-derived xenografts (PDX) and primary prostate cancer.

*(**A**) Scoring of Sigma-3 viral protein in ex vivo infected human prostate cancer tissue slices indicated heterogeneous response to exposure to 10^8 p.f.u. jin-3 reovirus. (**B**) Scoring of Sigma-3 viral protein in ex vivo infected primary prostate cancer material with 10^8 jin-3 reovirus for 4 days. Green viral capsid protein Sigma-3, red pan-cytokeratin or AMACR (tumour cell markers), blue DAPI (nuclei). Magnification is 63×, scale bar = 25 µm.*

Reovirus mutant jin-3 induces oncolysis in prostate cancer xenografts in vivo
Intra-tumoural administration of reovirus mutant *jin-3* reovirus in subcutaneously growing tumours from PC-3M-Pro4luc2 significantly decreased tumour burden ($p = 0.0367$) and diminished tumour volume ($p = 0.06$; **Figure 5A-D**). Viral capsid protein RNA expression in tumour cells was significantly upregulated in *jin-3* reovirus-treated prostate tumours (S4 $p < 0.0001$; **Figure 5E**). In line with the tumour regression data, histological analyses revealed that *jin-3* reovirus-treated tumours were depleted of proliferating cancer cells, their tissue architecture was lost and histological tumour markers significantly decreased. Conversely, high levels of viral Sigma-3 protein were detected in *jin-3* reovirus-treated tumours (**Figure 5F**). Similar data were obtained with our novel prostate cancer PDX model PCa-15.01, in which intra-tumoural injection of *jin-3* reovirus significantly reduced tumour volume ($p = 0.0072$) and tumour weight ($p = 0.0373$; **Figure 5G, H)**. Likewise, *jin-3* reovirus-treated tumours displayed a strong induction of viral RNA S4 transcripts ($p < 0.0001$; **Figure 5I**). Histological evaluation indicated a complete loss of tumour tissue architecture after *jin-3* reovirus treatment (**Figure 5J**).

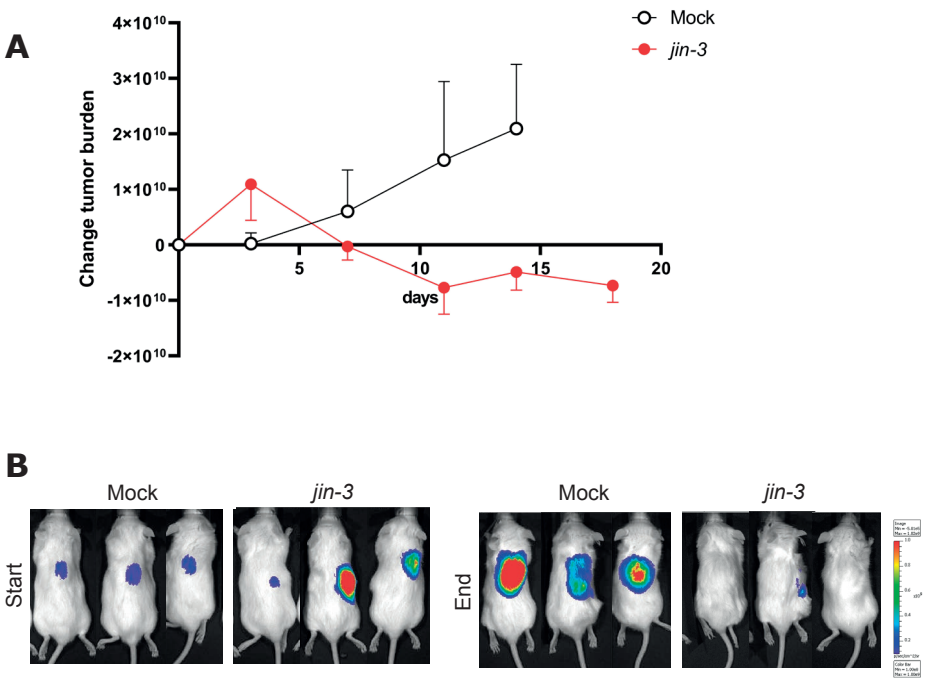

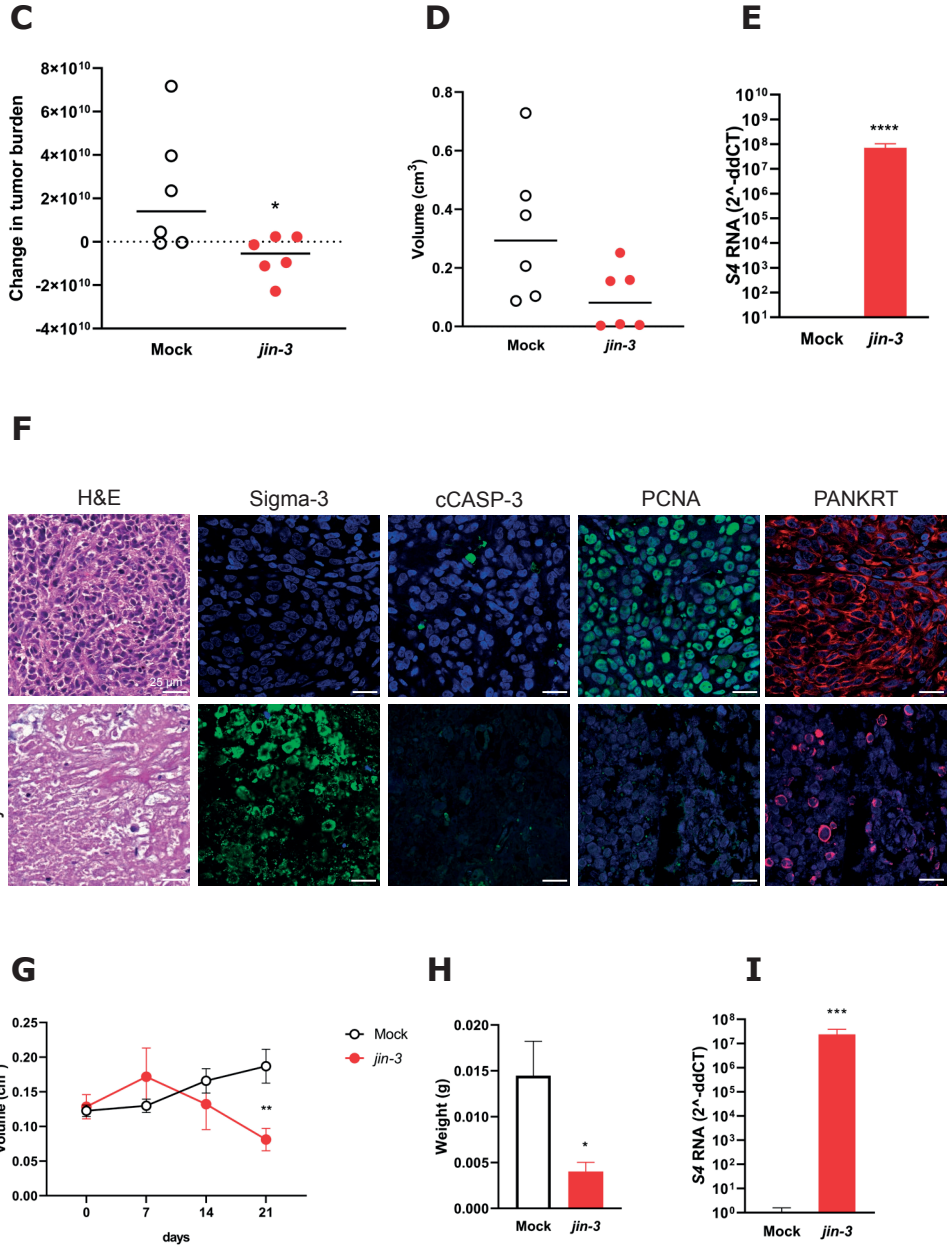
C
Change in tumor burden
8×10^10
6×10^10
4×10^10
2×10^10
0
-2×10^10
-4×10^10
*
Mock
jin-3
D
Volume (cm^3)
0.8
0.6
0.4
0.2
0.0
Mock
jin-3
E
S4 RNA (2^-ddCT)
10^10
10^9
10^8
10^7
10^6
10^5
10^4
10^3
10^2
10^1
****
Mock
jin-3
F
H&E
Sigma-3
cCASP-3
PCNA
PANKRT
Mock
jin-3
25 µm
G
Volume (cm^3)
0.25
0.20
0.15
0.10
0.05
0.00
0
7
14
21
days
**
Mock
jin-3
H
Weight (g)
0.020
0.015
0.010
0.005
0.000
*
Mock
jin-3
I
S4 RNA (2^-ddCT)
10^8
10^7
10^6
10^5
10^4
10^3
10^2
10^1
10^0
***
Mock
jin-3

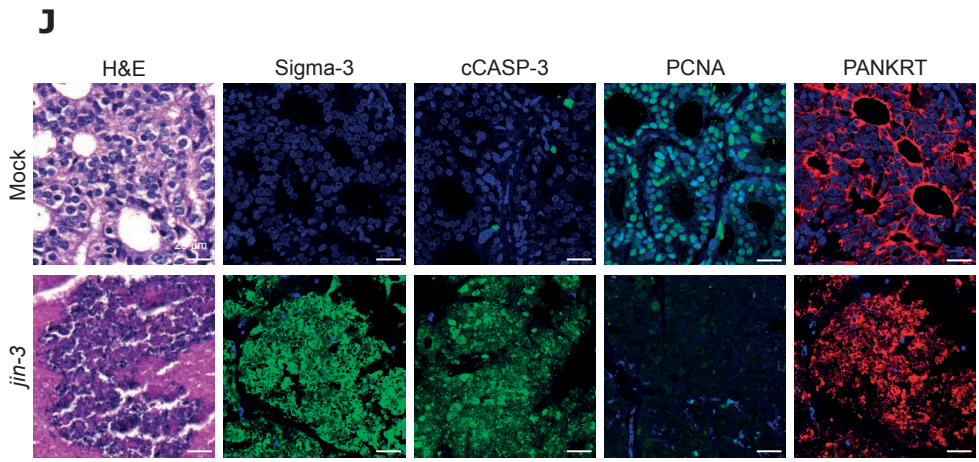

Figure 5 Direct oncolytic effects of *jin-3* reovirus in xenograft models of human prostate cancer models.

*The effect of intra-tumoural administration of jin-3 in subcutaneously growing human prostate tumours from cell line-derived xenograft (CDX) PC-3M-Pro4luc2 (**A–F**) and patient-derived xenograft (PDX) model PCa-15.01 (**G–J**). (**A**) Effect of jin-3 reovirus administration on total tumour burden was measured by whole-body bioluminescent reporter imaging (BLI) of firefly-luciferase2 expressing PC-3M-Pro4luc2 cells ($n = 6$ per group). (**B**) Whole-body bioluminescent optical imaging (BLI) at the start and end of the experiment. (**C**) Change of tumour burden (BLI) was significantly reduced in jin-3-treated tumours ($p < 0.05$). (**D**) Tumour volume (calliper measurements) was reduced after jin-3 administration. (**E**) S4 RNA expression, indicative of viral Sigma-3 gene expression, was observed in PC-3M-Pro4luc2 tumours treated with jin-3 reovirus at day 21 ($p < 0.0001$). (**F**) Histological evaluation depicted a strong oncolytic response, the presence of viral proteins (Sigma-3), a reduction in tumour cell proliferation (PCNA), and a loss of cytokeratins in PC-3M-Pro4luc2 tumours treated with jin-3 reovirus. (**G**) Treatment with jin-3 reovirus significantly reduced tumour volume in the PCa-15.01 PDX model ($n = 10$ per group; $p < 0.01$). (**H**) Significant tumour shrinkage upon intra-tumoural jin 3 administration (tumour weight; $p < 0.05$). (**I**) In tumours treated with jin-3 reovirus, viral S4 RNA was detected ($p < 0.0001$). (**J**) Histological evaluation of jin-3 reovirus-mediated anti-tumour effects indicated a loss of tissue architecture, the presence of viral proteins (Sigma-3), an induction of apoptosis (cleaved caspase-3), a reduction in proliferation (PCNA), and a loss of tumour-associated cytokeratins (PANKRT). Magnification is 63×, scale bar = 25 µm. Error bars indicated ± SEM, *$p < 0.05$, **$p < 0.01$, ***$p < 0.001$, ****$p < 0.0001$, two-way ANOVA and t tests.*

jin-3 reovirus induces determinants of immune modulation in human prostate cancer cells

Type I interferons and interferon-stimulated genes (ISGs) are of crucial importance in oncolytic virotherapy, as expression of ISGs associated with the sensitivity to oncolytic virotherapy (24, 25) (**Figure 6A**). Exposure to *jin-3* reovirus resulted in the significant upregulation of IFNβ gene expression in human prostate cancer cells after 48 h (**Figure 6B**). Compared to R124, exposure to *jin-3* reovirus resulted in a significant stronger induction in IFNβ gene expression ($^{\$}p < 0.05$; **Figure 6B**). Moreover, exposure of the cancer cells to *jin-3* reovirus resulted in a stronger induction of multiple ISGs compared to R124 (**Figure 6C**). Furthermore, treatment with *jin-3* reovirus induced a significant, dose-dependent induction of the inflammatory cytokines CXCL10, TNFα, and IL-1β. In addition, exposure to *jin-3* induced a significant stronger expression of CXCL10 and IL-1β compared to R124 ($^{\$\$\$}p < 0.001$ and $^{\$\$\$\$}p < 0.0001$). Expression of DDX58 that encodes for the cytosolic RNA sensor RIG-I, was also found to be significantly upregulated upon *jin-3* reovirus administration (**Figure 6D**). In addition, shedding of HMGB1 protein, a well-established marker for immunogenic cell death, was observed after exposure of prostate cancer cells to *jin-3* reovirus (26) (**Figure 6E)**. Moreover, additional upstream targets of the anti-viral response were significantly affected by *jin-3* reovirus exposure, including IFNAR1 and IFNAR2 (**Supplementary figure 5**).

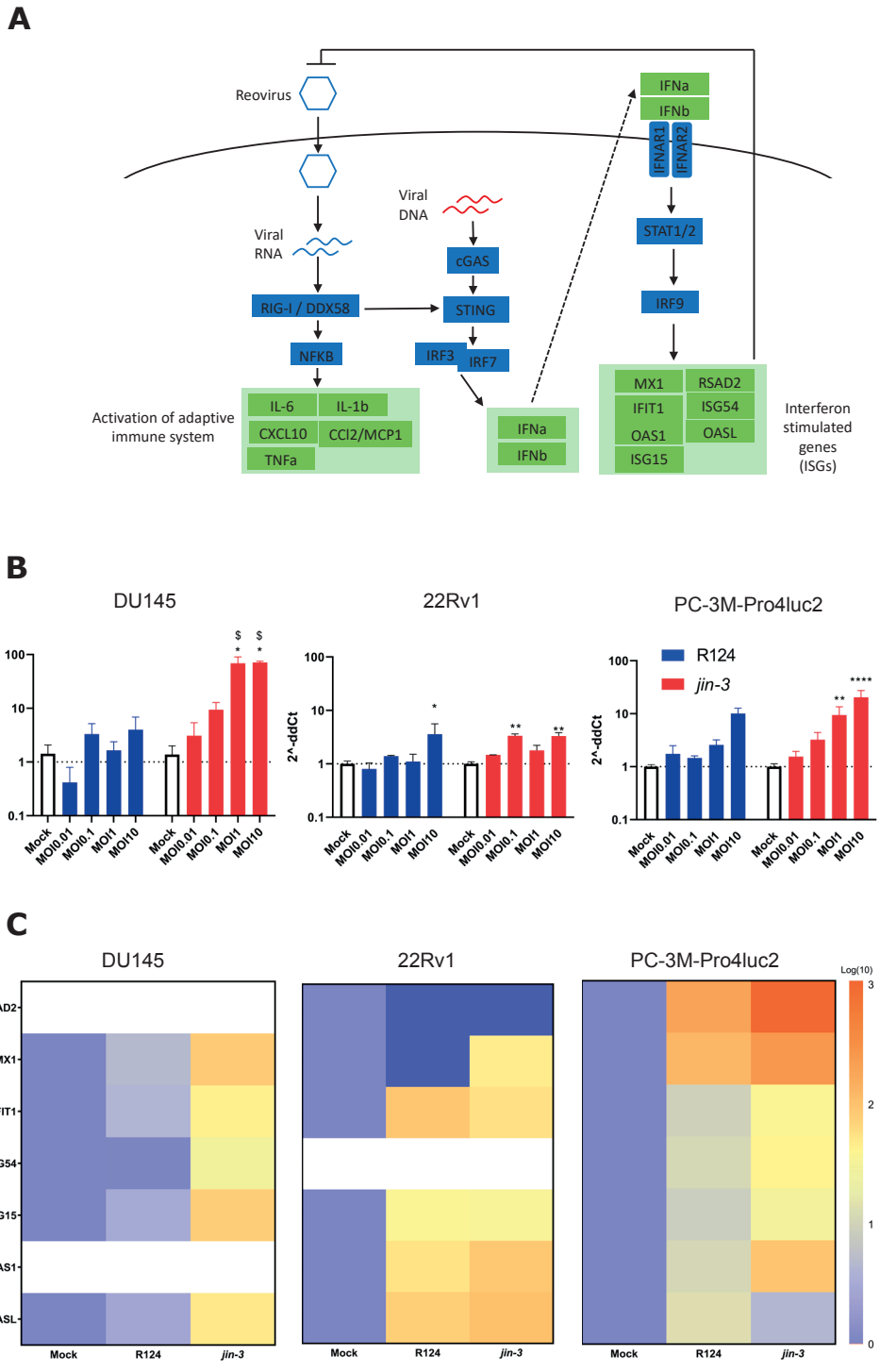
A
Reovirus
Viral RNA
Viral DNA
RIG-I / DDX58
cGAS
STING
NFKB
IRF3
IRF7
IFNa
IFNb
IFNAR1
IFNAR2
STAT1/2
IRF9
MX1
RSAD2
IFIT1
ISG54
OAS1
OASL
ISG15
IL-6
IL-1b
CXCL10
CCl2/MCP1
TNFa
Activation of adaptive immune system
Interferon stimulated genes (ISGs)
B
DU145
22Rv1
PC-3M-Pro4luc2
2^-ddCt
R124
jin-3
Mock
MOI0.01
MOI0.1
MOI1
MOI10
C
DU145
22Rv1
PC-3M-Pro4luc2
RSAD2
MX1
IFIT1
ISG54
ISG15
OAS1
OASL
Mock
R124
jin-3
Log(10)

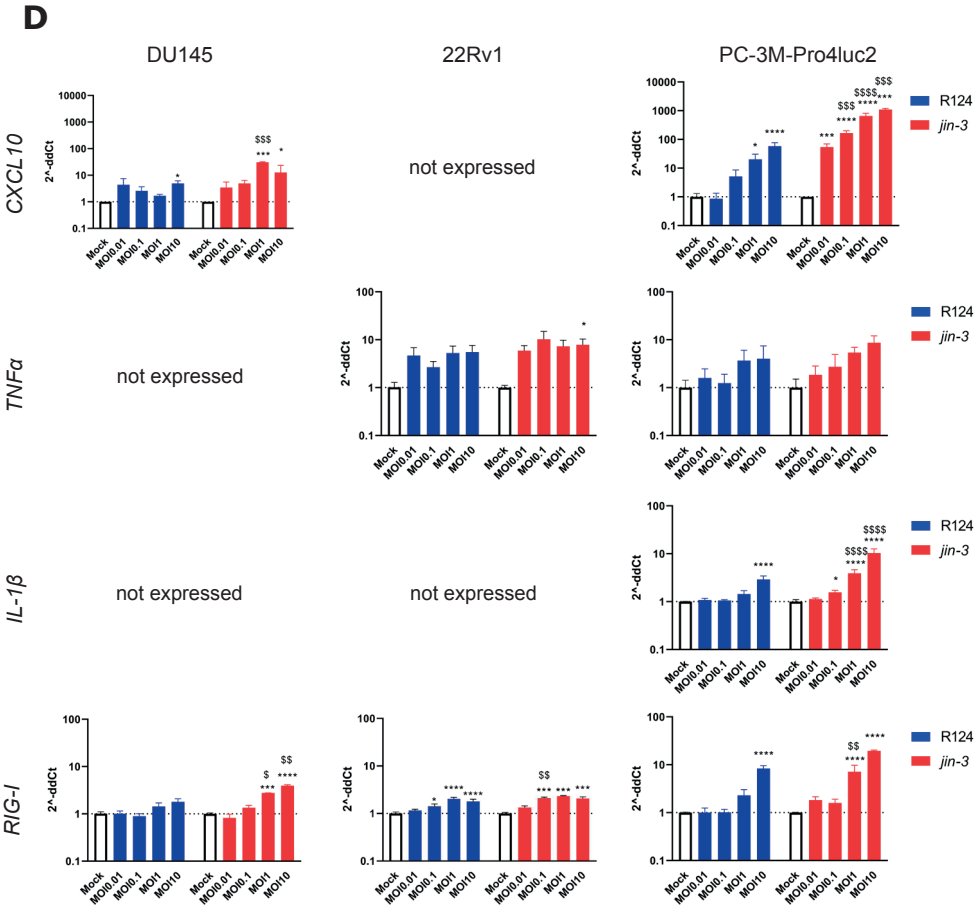
D
DU145
22Rv1
PC-3M-Pro4luc2
CXCL10
TNFα
IL-1β
RIG-I
not expressed
not expressed
not expressed
2^-ddCt
Mock
MOI0.01
MOI0.1
MOI1
MOI10
R124
jin-3

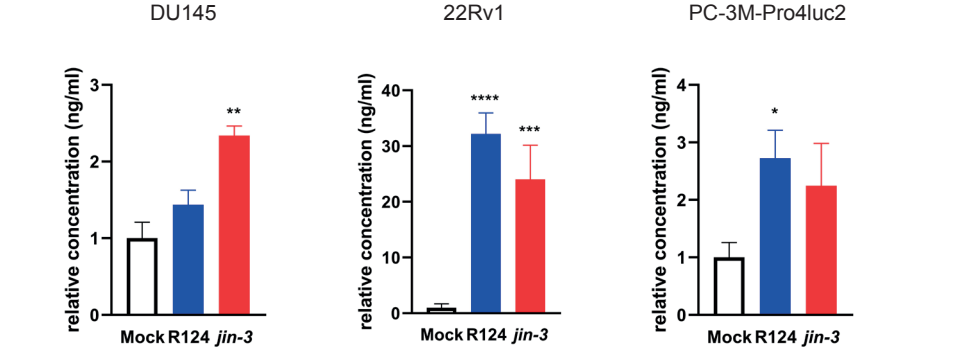
E
DU145
22Rv1
PC-3M-Pro4luc2
relative concentration (ng/ml)
Mock R124 jin-3

◄ Figure 6 Immune modulatory response of R124 parental and *jin-3* mutant reovirus in prostate cancer cultures.

*(**A**) The role of the STING pathway and IFN signalling in recognising viral RNA and induction of anti-viral and anti-tumour immune responses. (**B**) Induction of IFNβ mRNA in prostate cancer cells after treatment with R124 or jin-3 reovirus for 48 h.*

*(**C**) Induction of interferon-stimulated genes (ISGs) in human prostate cancer cells after treatment with MOI10 of R124 or jin-3 reovirus for 48 h (log-transformed). White boxes indicated that the gene was not expressed. (**D**) Induction of inflammatory cytokines gene expression of CXCL10, TNFα, and IL-1β and cytosolic RNA sensor RIG-I after treatment of human prostate cancer cells with reovirus. (**E**) HMGB1 protein release (danger-associated molecular pattern) by human prostate cancer cells after 48 h treatment with oncolytic reovirus. *$p < 0.05$, **$p < 0.01$, ***$p < 0.001$,****$p < 0.0001$, $^{\$}p < 0.05$, $^{\$\$}p < 0.01$, $^{\$\$\$}p < 0.001$, $^{\$\$}p < 0.0001$. Mean ± standard error of the mean (SEM), N = 2. Two-way ANOVA.*

Discussion

Current clinical and preclinical evidence demonstrates that anti-tumour immune responses can eliminate existing malignant cells, resulting in the protection against tumour recurrence (27, 28). However, the majority of prostate tumours does not adequately respond to immune therapy, which is mediated—among others—by the immunosuppressive tumour microenvironment, the low mutation burden resulting in limited expression of neoantigens, and immune evasion and exclusion processes in prostate tumours (4, 8, 29).

Oncolytic viruses are increasingly being exploited to counteract these immunosuppressive mechanisms by selectively killing cancer cells and, more importantly perhaps, by the initiation of anti-tumour immunity. Oncolytic viruses either have a natural preference to enter, replicate in, and/or kill cancer cells as opposed to normal cells or they are engineered to do so (30). To achieve improved anti-tumour immunity in prostate cancer, the identification and clinical development of optimised oncolytic viruses, alone or combined with other treatment modalities, may be advantageous. Here we report, for the first time, the use of *jin-3* reovirus in human prostate cancer models. Reovirus mutant *jin-3* reovirus induces potent direct anti-tumour effects in human prostate cancer. In ex vivo cultured human prostate cancer tissue slices and 2D/3D cell cultures, we found that *jin-3* reovirus is able to infect and replicate in the cancer cells. Moreover, *jin-3* reovirus exposure significantly induced the expression of ISGs and inflammatory cytokines. This is further substantiated by the release of immunogenic cell death marker HMGB1 after exposure of cancer cells to *jin-3* reovirus.

A number of preclinical studies have reported the anti-tumour effects of wild-type mammalian Orthoreovirus (31, 32). In addition, clinical trials have revealed that wild-type reovirus has inherent oncolytic properties, is not associated with serious human disease, and has a favourable safely profile in cancer patients (11). However, clinical trials have demonstrated that the clinical benefit of wild-type reovirus administration in prostate cancer patients is limited and so far phase II studies have revealed no survival benefit (11, 12, 32, 33, 34, 35, 36).

We previously described the isolation of reoviruses with an expanded tropism (10). These so-called *jin* mutant reoviruses can also infect cancer cells independently of the canonical reovirus entry receptor JAM-A (10). The potential oncolytic and immunomodulatory properties of these mutant reoviruses were not previously established in preclinical models of human prostate cancer. Here, we show that the reovirus mutant *jin-3* displays strong oncolytic and immunomodulatory properties and represents an interesting candidate oncolytic virus for the treatment of prostate cancers. We observed efficacious *jin-3* infection in the majority of ex vivo cultured prostate cancer tissue slices derived from PDXs and primary prostate cancer patient material. Moreover, *jin-3* induced significant tumour regression in various human prostate cancer xenografts in vivo as indicated by real-time optical imaging measurements (firefly luciferase2 expressing cancer cells) to determine the total tumour burden, changes in tumour volume, tumour weight, and reduction of pan-cytokeratin. In prolonged in vivo experiments and in a clinical setting, it will also be worthwhile to assess the effect of *jin-3*. Reovirus exposure on additional tumour markers in circulation, e.g., serum PSA. In this study, we observed that *jin-3* reovirus administration induces several ISGs and inflammatory cytokines. The *jin-3* reovirus-induced gene expression of key immunomodulators (activators of the adaptive and innate immune system) is further substantiated by the release of HMGB1 as one of the key DAMPs.

In conclusion, we describe the evaluation as an oncolytic agent of the mutant reovirus *jin-3* that displays strong oncolytic and immunomodulatory properties in state-of-the-art preclinical prostate cancer models, including patient-derived tumour slice models. Our findings support the notion that *jin-3* reovirus can be potentially exploited in strategic treatment combinations to with otherwise less efficacious immuno-oncological or chemotherapeutical approaches to achieve improved and durable anti-tumour responses.

Acknowledgments

This study was supported by a personalised medicine grant from the Dutch Cancer Society (KWF) Alpe D'HuZes (UL2014-7058), OAK Foundation (SOAK 18.01 and SOAK-Strati-Vir project), and a kind gift from the Franje Foundation.

References

1. Bray F, Ferlay J, Soerjomataram I, Siegel RL, Torre LA, Jemal A. Global cancer statistics 2018: GLOBOCAN estimates of incidence and mortality worldwide for 36 cancers in 185 countries. CA Cancer J Clin. 2018;68:394–424.

2. Tang J, Shalabi A, Hubbard-Lucey VM. Comprehensive analysis of the clinical immuno-oncology landscape. Ann Oncol. 2018;29:84–91.

3. Bilusic M, Madan RA, Gulley JL. Immunotherapy of prostate cancer: facts and hopes. Clin Cancer Res. 2017;23:6764–70.

4. Vitkin N, Nersesian S, Siemens DR, Koti M. The tumor immune contexture of prostate cancer. Front Immunol. 2019;10:603.

5. Davola ME, Mossman KL. Oncolytic viruses: how "lytic" must they be for therapeutic efficacy? Oncoimmunology. 2019;8:e1581528.

6. Errington F, Steele L, Prestwich R, Harrington KJ, Pandha HS, Vidal L, et al. Reovirus activates human dendritic cells to promote innate antitumor immunity. J Immunol. 2008;180:6018–26.

7. Prestwich RJ, Errington F, Steele LP, Ilett EJ, Morgan RS, Harrington KJ, et al. Reciprocal human dendritic cell-natural killer cell interactions induce antitumor activity following tumor cell infection by oncolytic reovirus. J Immunol. 2009;183:4312–21.

8. Lee P, Gujar S. Potentiating prostate cancer immunotherapy with oncolytic viruses. Nat Rev Urol. 2018;15:235–50.

9. Kemp V, Lamfers MLM, van der Pluijm G, van den Hoogen BG, Hoeben RC. Developing oncolytic viruses for clinical use: A consortium approach. Cytokine Growth Factor Rev. 2020;56:133–40.

10. van den Wollenberg DJ, Dautzenberg IJ, van den Hengel SK, Cramer SJ, de Groot RJ, Hoeben RC. Isolation of reovirus T3D mutants capable of infecting human tumor cells independent of junction adhesion molecule-A. PLoS ONE. 2012;7:e48064.

11. Vidal L, Pandha HS, Yap TA, White CL, Twigger K, Vile RG, et al. A phase I study of intravenous oncolytic reovirus type 3 Dearing in patients with advanced cancer. Clin Cancer Res. 2008;14:7127–37.

12. Thirukkumaran CM, Nodwell MJ, Hirasawa K, Shi ZQ, Diaz R, Luider J, et al. Oncolytic viral therapy for prostate cancer: efficacy of reovirus as a biological therapeutic. Cancer Res. 2010;70:2435–44.

13. Barton ES, Forrest JC, Connolly JL, Chappell JD, Liu Y, Schnell FJ, et al. Junction adhesion molecule is a receptor for reovirus. Cell. 2001;104:441–51.

14. Zhao C, Lu F, Chen H, Zhao X, Sun J, Chen H. Dysregulation of JAM-A plays an important role in human tumor progression. Int J Clin Exp Pathol. 2014;7:7242–8.

15. van de Merbel AF, van der Horst G, van der Pluijm G. Patient-derived tumour models for personalized therapeutics in urological cancers. Nat Rev Urol. 2021;18(1):33–45.

16. Dautzenberg IJ, van den Wollenberg DJ, van den Hengel SK, Limpens RW, Barcena M, Koster AJ, et al. Mammalian orthoreovirus T3D infects U-118 MG cell spheroids independent of junction adhesion molecule-A. Gene Ther. 2014;21:609–17.

17. Gao D, Vela I, Sboner A, Iaquinta PJ, Karthaus WR, Gopalan A, et al. Organoid cultures derived from patients with advanced prostate cancer. Cell. 2014;159:176–87.

18. Drost J, Karthaus WR, Gao D, Driehuis E, Sawyers CL, Chen Y, et al. Organoid culture systems for prostate epithelial and cancer tissue. Nat Protoc. 2016;11:347–58.

19. van de Merbel AF, van der Horst G, van der Mark MH, van Uhm JIM, van Gennep EJ, Kloen P, et al. An ex vivo tissue culture model for the assessment of individualized drug responses in prostate and bladder cancer. Front Oncol. 2018;8:400.

20. Navone NM, van Weerden WM, Vessella RL, Williams ED, Wang Y, Isaacs JT, et al. Movember GAP1 PDX project: An international collection of serially transplantable prostate cancer patient-derived xenograft (PDX) models. Prostate. 2018;78:1262–82.

21. van den Hoogen C, van der Horst G, Cheung H, Buijs JT, Lippitt JM, Guzman-Ramirez N, et al. High aldehyde dehydrogenase activity identifies tumor-initiating and metastasis-initiating cells in human prostate cancer. Cancer Res. 2010;70:5163–73.

22. van Weerden WM, de Ridder CM, Verdaasdonk CL, Romijn JC, van der Kwast TH, Schroder FH, et al. Development of seven new human prostate tumor xenograft models and their histopathological characterization. Am J Pathol. 1996;149:1055–62.

23. Marques RB, Dits NF, Erkens-Schulze S, van Weerden WM, Jenster G. Bypass mechanisms of the androgen receptor pathway in therapy-resistant prostate cancer cell models. PLoS ONE. 2010;5:e13500.

24. Matveeva OV, Chumakov PM. Defects in interferon pathways as potential biomarkers of sensitivity to oncolytic viruses. Rev Med Virol. 2018;28:e2008.

25. Kurokawa C, Iankov ID, Anderson SK, Aderca I, Leontovich AA, Maurer MJ, et al. Constitutive interferon pathway activation in tumors as an efficacy determinant following oncolytic virotherapy. J Natl Cancer Inst. 2018;110:1123–32.

26. Kepp O, Senovilla L, Vitale I, Vacchelli E, Adjemian S, Agostinis P, et al. Consensus guidelines for the detection of immunogenic cell death. Oncoimmunology. 2014;3:e955691.

27. Waldman AD, Fritz JM, Lenardo MJ. A guide to cancer immunotherapy: from T cell basic science to clinical practice. Nat Rev Immunol. 2020;20(11):651–68.

28. Garner H, de Visser KE. Immune crosstalk in cancer progression and metastatic spread: a complex conversation. Nat Rev Immunol. 2020;20:483–97.

29. Silvestri I, Cattarino S, Aglianò AM, Collalti G, Sciarra A. Beyond the immune suppression: the immunotherapy in prostate cancer. Biomed Res Int. 2015;2015:794968.

30. Kemp V, Lamfers MLM, van der Pluijm G, van den Hoogen BG, Hoeben RC. Developing oncolytic viruses for clinical use: A consortium approach. Cytokine Growth Factor Rev. 2020;56:133–40.

31. Thirukkumaran CM, Shi ZQ, Luider J, Kopciuk K, Gao H, Bahlis N, et al. Reovirus as a viable therapeutic option for the treatment of multiple myeloma. Clin Cancer Res. 2012;18:4962–72.

32. Heinemann L, Simpson GR, Boxall A, Kottke T, Relph KL, Vile R, et al. Synergistic effects of oncolytic reovirus and docetaxel chemotherapy in prostate cancer. BMC Cancer. 2011;11:221.

33. Gujar SA, Pan DA, Marcato P, Garant KA, Lee PW. Oncolytic virus-initiated protective immunity against prostate cancer. Mol Ther. 2011;19:797–804.

34. Comins C, Spicer J, Protheroe A, Roulstone V, Twigger K, White CM, et al. REO-10: a phase I study of intravenous reovirus and docetaxel in patients with advanced cancer. Clin Cancer Res. 2010;16:5564–72.

35. Eigl BJ, Chi K, Tu D, Hotte SJ, Winquist E, Booth CM, et al. A randomized phase II study of pelareorep and docetaxel or docetaxel alone in men with metastatic castration resistant prostate cancer: CCTG study IND 209. Oncotarget. 2018;9:8155–64.

36. Berkeley RA, Steele LP, Mulder AA, van den Wollenberg DJM, Kottke TJ, Thompson J, et al. Antibody-neutralized reovirus is effective in oncolytic virotherapy.

Supplementary table 1 Cell culture media.

Cell line	RRID	Medium	Supplier	Supplements
PC-3M-Pro4luc2		Dulbecco's Modified Eagle medium (DMEM)	Life Technologies, Gibco, 31966-021	10% FCII (Hyclone), 100 units/ml penicillin, 50 µg/ml Streptomycin, 800 µg/ml of G-418
DU145	ATCC Cat# HTB-81, RRID: CVCL_0105	RPMI-1640	Lonza, BE12-167F	10% FBS, 100 units/ml penicillin, 50 µg/ml Streptomycin, GlutaMAX
22Rv1	ATCC Cat# 2505, RRID: CVCL_1045	RPMI-1640	Lonza, BE12-167F	10% FBS, 100 units/ml penicillin, 50 µg/ml Streptomycin, GlutaMAX

Supplementary table 2 Antibodies used for immunofluorescence stainings and FACS analysis.

Target	Species	Supplier	Dilution	Assay
4F2 against reovirus σ3	Mouse	Antibody was develoed by T.S. Dermody [36]; purchased at the Developmental Studies Hybridoma Bankd developed under the auspices of the NICHD and maintained by The University of Iowa, Department of Biology, Iowa City, IA52242	1:200	ICC, IF
Pan cytokeratin	Rabbit	Abcam ab217916	1:500	IF
Collagen type I	Goat	Southern Biotech No 1310-01	1:1000	IF
AMACR	Rabbit	Atlas antibody HPA019527	1:5000	IF
PCNA	Mouse	Sigma Aldrich P8825	1:2000	IF
Cleaved caspase-3	Rabbit	Cell Signaling 9961:	1:500	IF
JAM-A	Mouse	Abnova H00050848-M01	1:250	IF
JAM-A	Mouse	Abcam ab17261	1:200	FACS
AR	Rabbit	Cell Signaling 5153	1:500	IF

Supplementary table 2 (continued) Antibodies used for immunofluorescence stainings and FACS analysis.

Target	Species	Supplier	Dilution	Assay
Donkey anti-mouse Alexa Fluor 488	Donkey	Life Technologies A-21202	1:250	ICC, IF, FACS
Donkey anti-rabbit Alexa Fluor 488	Donkey	Life Technologies A-21206	1:250	IF
Donkey anti-mouse Alexa Fluor 555	Donkey	Life Technologies A-31570	1:250	IF
Donkey anti-rabbit Alexa Fluor 555	Donkey	Life Technologies A-31572	1:250	IF
Donkey anti-goat Alexa Fluor 647	Donkey	Life Technologies A-21447	1:250	IF

Supplementary table 3 Characteristics of newly generated patient-derived xenograft models and primary prostate cancer biopsies.

Novel established models and patient biopsies used for ex vivo cultures					
Sample name	**Source**	**TNM stage**	**Gleason Grade**	**PSA (µg/ml)**	**Treatment history**
PCa-15.01	Prostatectomy (hormone naive)	T3NxM+	4+5	>5000	No previous treatment
NM60	Needle biospy liver metastasis (CRPC)	N.A.	N.A.	81.0	Zoladex, Docetaxel, Abiraterone, ratiotherapy, Cabazitaxel, Carboplatin, Olaparib
NM72	Needle biopsy liver metastasis (CRPC)	M1c	N.A.	51.0	Prostatectomy, Docetaxel, Abiraterone, Cabazitaxel, Olaparib, Cabazitaxel/ Carboplatin
NM78	Prostate cancer bone metastasus	M1b	N.A.	470.0	EBRT, Androgen deprivation (Eligard), Enzalutamide, Abiraterone

Supplementary table 3 (Continued) Characteristics of newly generated patient-derived xenograft models and primary prostate cancer biopsies.

Sample name	Source	TNM stage	Gleason Grade	PSA (µg/ml)	Treatment history
Patient #1	Transurethral resection	T4N+M+	4+4	52.5	EBRT, LHRH agonist, Enzalutamide
Patient #2	Transurethral resection	T3bNxMx	3+4	7.5	LHRH agonist
Patient #3	Transurethral resection	T3bN0Mx	4+4	15.0	Androgen deprivation
Patient #4	Transurethral resection	T3bN+M+	5+5	1.58	LHRH agonist, Enzalutamide
Paatient #6	Transurethral resction	T4N1M1b	5+5	29.36	Bicaluamide, Zoladex
Patient #7	Transurethral resection	T3aN0M0	4+5	14.23	EBRT, Bicalutamide, Goserelin
Patient #8 (NM91)	Prostate cancer bone metastasis	M1b	N.A.	21.0	Prostatectomy, EBRT, Docetaxel, Enzalutamide, Talazoparib, ongoing bone resection

Supplementary table 4 Characteristics of previously established three-dimensional cultures and patient-derived xenograft lines.

Previously established models					
Tumour model	**Source**	**Treatment history**	**Clinical status**	**Diagnosis**	**Refs**
MSK-PCa1	L2 vertebral body	Androgen-deprivation therapy, bicalutamide	mCRPC	Intraductal carcinoma	(17)
MSK-PCa2	Acetabulum	Androgen-deprivation therapy, bicalutamide	mCRPC	Adeno-carcinoma	(17)
PC82	Radical prostatectomy	No previous treatment	Hormone naive	Adeno-carcinoma	(20, 22)
PC295	Lymph node resection	None	Hormone naive	Adeno-carcinoma	(20, 22)
PC310	Radical prostatectomy	None	Hormone naive	Adeno-carcinoma	(20, 22)
PC324	Transurethral resection	Bilateral orchiectomy	mCRPC	Adeno-carcinoma and neuro-endocrine differentiation	(20, 22)
PC339C	Transurethral resection	LHRH agonist	mCRPC	Adeno-carcinoma	(20, 22)
PC346C	Transurethral resction	Anti-androgen	Hormone responsive	Adeno-carcinoma	(22, 23)
PC374	Scrotal skin metastasis biopsy	Androgen-deprivation, radiotherapy, anti-androgen	mCRPC	Adeno-carcinoma	(20, 22)

Supplementary table 5 Primer sequences used for RTqPCR.

Target	Primer sequence
Mycoplasma A1	TGCACCATCTGTCACTCTGTTAACCTC
Mycoplasma A2	GGGAGCAAACAGGATTAGATACCCT
Human GAPDH FW	GACAGTCAGCCGCATCTTC
Human GAPDH RV	GCAACAATATCCACTTTACCAGAG
Universal GAPDH FW	CCATGGAGAAGGCTGGGG
Universal GAPDH RV	CAAAGTTGTCATGGATGACC
MX1 FW	TCAGCACCTGATGGCCTA
MX1 RV	AAAGGGATGTGGCTGGAGAT
OASL FW	TTGCTATGACAACAGGGAGAAC
OASL RV	CTGTCAAGTGGATGTCTCGTG
DDX58 FW	TGTGGGCAATGTCATCAAAA
DDX58 RV	GAAGCACTTGCTACCTCTTGC
CXCL10 FW	GAAAGCAGTTAGCAAAGGAAAGGT
CXCL10 RV	GACATATACTCCATGTAGGGAAGTGA
RSAD2 FW	TGCTTTTGCTTAAGGAAGCTG
RSAD2 RV	AGGTATTCTCCCCGGTCTTG
ISG54 FW	ATATAGGTCTCTTCAGCATTTATTGGT
ISG54 RV	CAAGGAATTCTTATTGTTCTCACTCA
TNFa FW	CAGCCTCTTCTCCTTCCTGAT
TNFa RV	GCCAGAGGGCTGATTAGAGA
IL1B FW	TACCTGTCCTGCGTGTTGAA
IL1B RV	TCTTTGGGTAATTTTTGGGATCT
IFNAR1 FW	ATTTACACCATTTCGCAAAGC
IFNAR1 RV	CACTATTGCCTTATCTTCAGCTTCTA
IFNAR2 FW	TAGCCTCCCCAAAGTCTTGA
IFNAR2 RV	AAATGACCTCCACCATATCCA
ISG15 FW	GCGAACTCATCTTTGCCAGTA
ISG15 RV	CCAGCATCTTCACCGTCAG
IFIT1 FW	GCCTAATTTACAGCAACCATGA
IFIT1 RV	CAAGGAATTCTTATTGTTCTCACTCA
IFNB FW	CTTTGCTATTTTCAGACAAGATTCA
IFNB RV	GCCAGGAGGTTCTCAACAAT
S4Q FW	CGCTTTTGAAGGTCGTGTATCA
S4Q RV	CTGGCTGTGCTGAGATTGTTTT

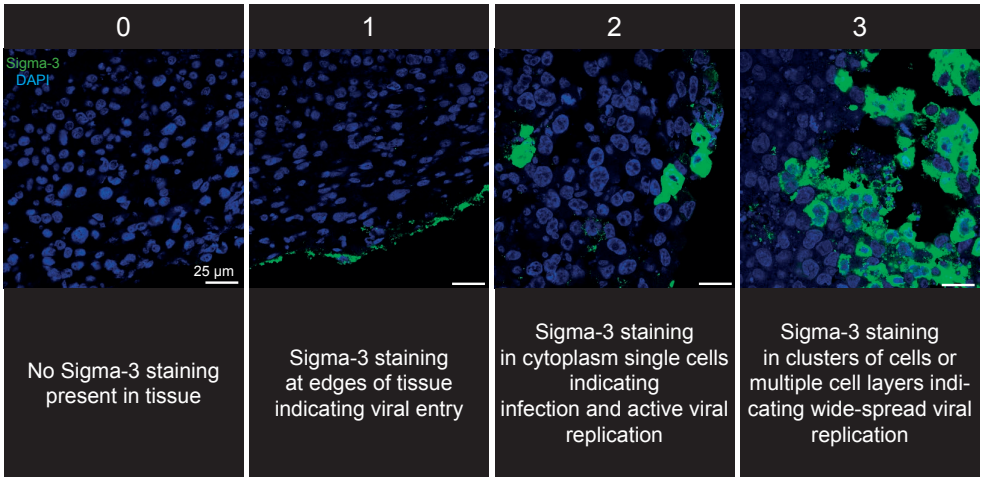

Supplementary figure 1 Sigma-3 scoring system.

Prostate cancer tissue slices exposed to reovirus were stained with an antibody directed against viral protein Sigma-3 and scored according to Sigma-3 pattern ranging from 0 to 3.

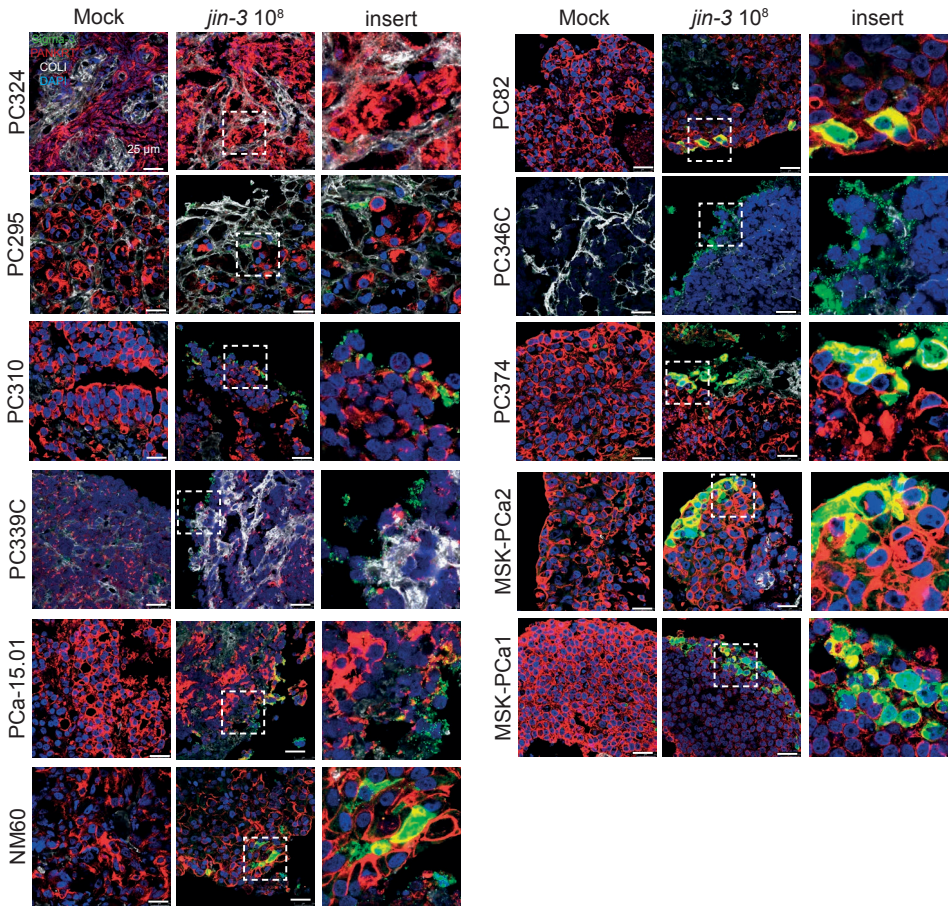

Supplementary figure 2 Sigma-3 staining in prostate cancer tissue slices derived from PDX models upon reovirus exposure.

Sigma-3 (green), pan-cytokeratin (red), type I collagen (white), DAPI (blue) staining in human prostate cancer tissue slices derived from PDX models. Prostate cancer tissue slices were ex vivo exposed to 10^8 pfu/ml reovirus for 3 days. Magnification is 63x, scale bar = 25 µm

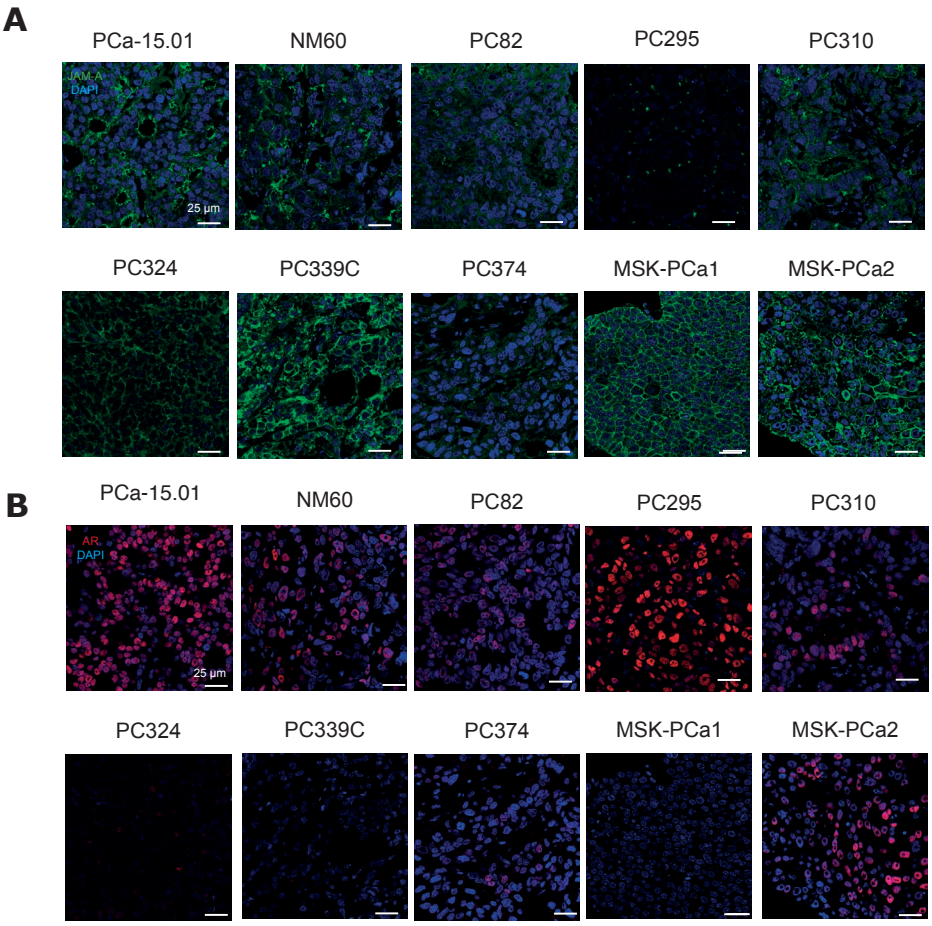

Supplementary figure 3 JAM-A and AR expression in prostate cancer patient-derived xenograft (PDX) models.

*Immunolocalisation of reovirus entry receptor junction adhesion molecule-A (JAM-A) (**A**) and the androgen receptor (AR) (**B**) in a broad spectrum of human prostate cancer PDX tissues (green). Magnification is 63x, scale bar = 25 µm*

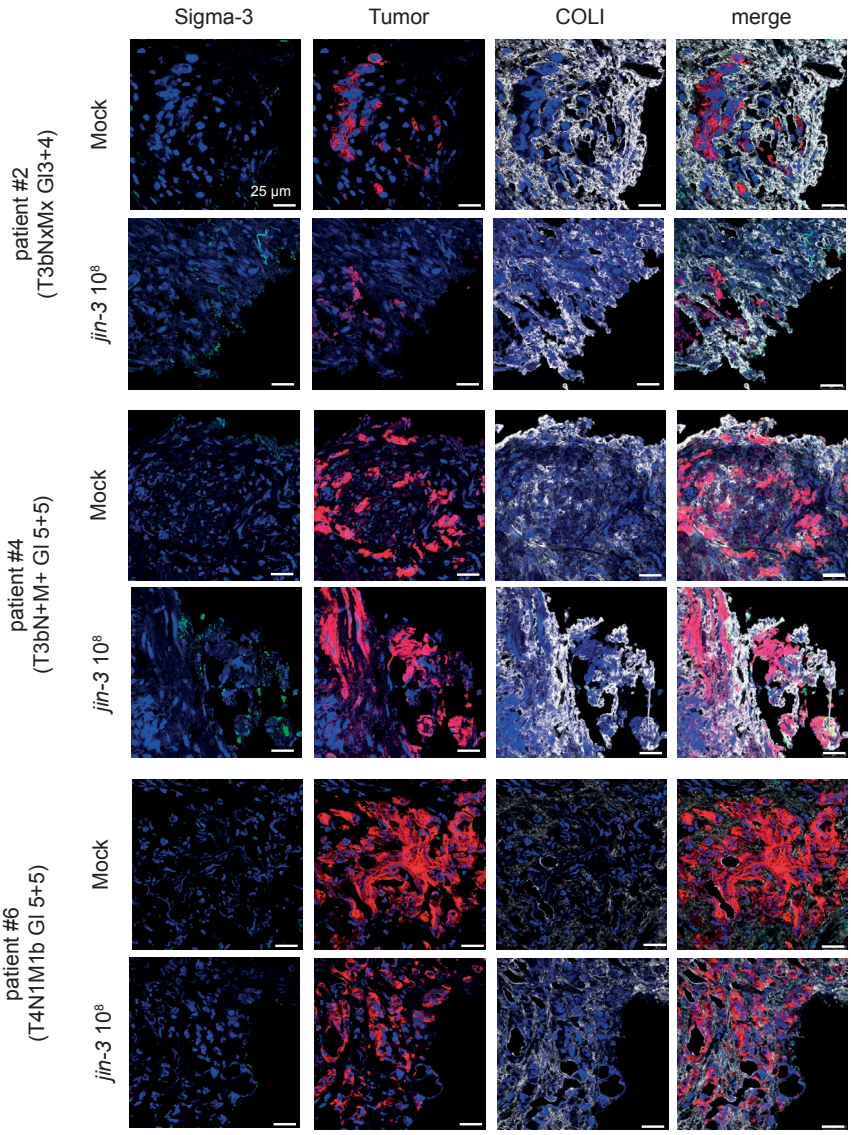
Sigma-3
Tumor
COLI
merge
patient #2
(T3bNxMx Gl3+4)
Mock
jin-3 10⁸
patient #4
(T3bN+M+ Gl 5+5)
Mock
jin-3 10⁸
patient #6
(T4N1M1b Gl 5+5)
Mock
jin-3 10⁸
25 µm

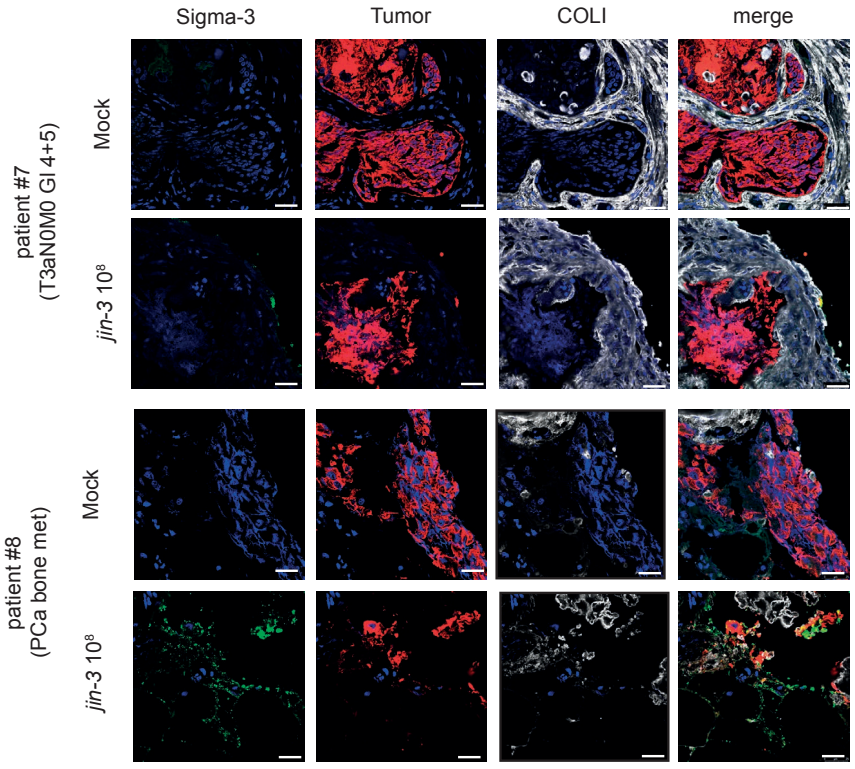

Supplementary figure 4 Sigma-3 staining in primary prostate cancer tissue slices derived from transurethral resection of the prostate upon reovirus exposure.

Sigma-3 (viral protein, green), pan-cytokeratin or AMACR (tumour cells, red), type I collagen fibres (white), DAPI (blue, nuclei) stainings in prostate cancer tissue slices derived from transurethral resection of the prostate primary samples. Prostate cancer tissue slices were ex vivo exposed to 108 pfu/ml reovirus for 3 days. Magnification is 63x, scale bar = 25 µm

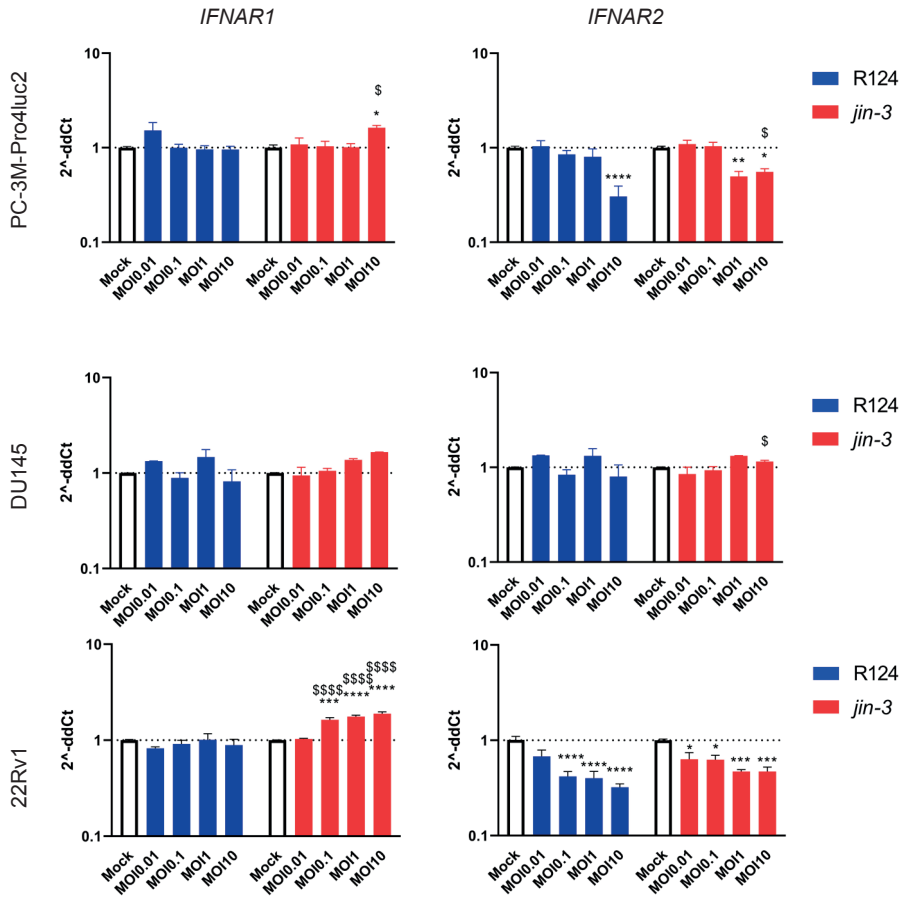

Supplementary figure 5 Changes in IFNAR1, IFNAR2 mRNA expression upon reovirus exposure.

*Infection with jin-3 changed mRNA expression of IRNAR1, IFNAR2 after 48h in human prostate cancer cells. * p<0.05, ** p<0.01, *** p<0.001, **** p<0.0001, $ p<0.05, $$ p<0.01, $$$ p<0.001, $$$$ p<0.0001. Mean +/- standard error of the mean (SEM), N=2. Two-way ANOVA. MOI = multiplicity of infection*

Supplementary information

Sample size
Sample size was chosen according to expected differences in the groups according to the following formula: n=2·(Z_((1-α/2))+Z_((1-β)))^2/Δ^2 Δ=(μ1-μ2)/σ.

(n= sample size , Z_((1-α/2)) = percentage points of the normal distribution for the statistical significance level, Z_((1-β))= percentage points of the normal distribution for the power, Δ= standardized difference, μ=mean, σ= standard deviation).

For calculation of the sample size for the androgen independent in vivo model (PC-3M-Pro4luc) we have used the relative light units measured with bioluminescent imaging. With expected mean value of the tumour burden is 3.5*10^9 RLU with a standard deviation of 1 *10^9. Expected difference is -45%. Power: 80%, significance level: 5%

For the androgen dependent in vivo model (PCa-15.01): we have calculated the sample size using the expected tumour volume. The expected mean value of the tumour burden is 1.5cm^3 with a standard deviation of 0.5cm^3. Expected difference is -45%. Power: 80%, significance level: 5%

Exclusion criteria
Pre-established exclusion criteria for the preclinical in vivo models: when tumour does not develop, the mouse will be excluded from the experiment. Further exclusion criteria for analysis of the data: when a mouse will reach humane endpoints before the end of the experiment, this mouse will be excluded from analysis.

No mice were excluded based on these criteria in our reported experiments.